10-27-2014

# Comparison of passive microwave and modeled estimates of total watershed SWE in the continental United States

Carrie M. Vuyovich
*U.S. Army Corps of Engineers*

Jennifer M. Jacobs
*University of New Hampshire, Durham*, jennifer.jacobs@unh.edu

Steven F. Daly
*Cold Regions Research and Engineering Laboratory*



Recommended Citation
Vuyovich*, C.M., J.M Jacobs and S.F. Daly. 2014. Comparison of passive microwave and SNODAS estimates of total watershed SWE in the continental U.S. Water Resources Research. doi: 10.1002/2013WR014734.

AGU PUBLICATIONS

Water Resources Research

RESEARCH ARTICLE
10.1002/2013WR014734

# Comparison of passive microwave and modeled estimates of total watershed SWE in the continental United States

**Carrie M. Vuyovich[1], Jennifer M. Jacobs[2], and Steven F. Daly[1]**

[1]Cold Regions Research and Engineering Laboratory, Hanover, New Hampshire, USA, [2]Department of Civil Engineering, University of New Hampshire, Durham, New Hampshire, USA

**Key Points:**
- Passive microwave SWE estimates compare well to SNODAS in regions with less than 20% forest and no more than 200 mm SWE
- In deep snow regions, passive microwave SWE estimates share the timing, but not the magnitude or rank-ordering of SNODAS
- Algorithm differences between SSM/I and AMSR-E seem to account for dissimilar performance in areas with dense vegetation or thin snow

**Correspondence to:**
C. M. Vuyovich,
carrie.m.vuyovich@usace.army.mil

**Citation:**
Vuyovich, C. M., J. M. Jacobs, and S. F. Daly (2014), Comparison of passive microwave and modeled estimates of total watershed SWE in the continental United States, *Water Resour. Res.*, *50*, 9088–9102, doi:10.1002/2013WR014734.

Received 18 SEP 2013
Accepted 20 OCT 2014
Accepted article online 27 OCT 2014
Published online 26 NOV 2014

**Abstract** In the U.S., a dedicated system of snow measurement stations and snowpack modeling products is available to estimate the snow water equivalent (SWE) throughout the winter season. In other regions of the world that depend on snowmelt for water resources, snow data can be scarce, and these regions are vulnerable to drought or flood conditions. Even in the U.S., water resource management is hampered by limited snow data in certain regions, as evident by the 2011 Missouri Basin flooding due in large part to the significant Plains snowpack. Satellite data could potentially provide important information in under-sampled areas. This study compared the daily AMSR-E and SSM/I SWE products over nine winter seasons to spatially distributed, modeled output SNODAS summed over 2100 watersheds in the conterminous U.S. Results show large areas where the passive microwave retrievals are highly correlated to the SNODAS data, particularly in the northern Great Plains and southern Rocky Mountain regions. However, the passive microwave SWE is significantly lower than SNODAS in heavily forested areas, and regions that typically receive a deep snowpack. The best correlations are associated with basins in which maximum annual SWE is less than 200 mm, and forest fraction is less than 20%. Even in many watersheds with poor correlations between the passive microwave data and SNODAS maximum annual SWE values, the overall pattern of accumulation and ablation did show good agreement and therefore may provide useful hydrologic information on melt timing and season length.

## 1. Introduction

Snow is an important source of water in many temperate regions of the world. In the mountainous, western U.S., snowmelt accounts for up to 75% of the annual streamflow [*Doesken and Judson*, 1996; *Daly et al.*, 2001]. Other regions of the U.S., for example, the Great Plains, do not rely as heavily on snow for water supply, but can still experience significant flooding as a result of snowmelt [*Todhunter*, 2001; *USACE*, 2012]. Water management in these regions requires accurate, timely estimates of snow water equivalent (SWE) for resource allocation and flood forecasting. However, validation of SWE estimates can be challenging given the heterogeneous and dynamic nature of snow, and the varying resolutions of measurements.

Satellite-based passive microwave sensors could provide spatially distributed snowpack information, particularly in remote, data-sparse regions because they have a twice-daily temporal resolution and the ability to see through clouds and at night. However, known sources of error prohibit the operational use of this data set in many regions. In regions, where heavy vegetation and significant snowpack depths do not impact the data, studies have shown promising results in the passive microwave estimates of SWE [*Dong et al.*, 2005]. In the Great Plains of the United States and the Canadian Plains where the algorithms were developed, SSM/I SWE compares well to ground observations [*Derksen et al.*, 2003; *Mote et al.*, 2003; *Chang et al.*, 2005]. *Tait* [1998] compared passive microwave SWE estimates to ground observations in the United States and Russia, categorized by land-cover, and found good agreement in nonforested, flat regions when wet snow or depth hoar was not affecting the microwave signal. *Vuyovich and Jacobs* [2011] found that passive microwave data provided reasonable estimates of SWE in the Upper Helmand Watershed in central Afghanistan. Modeled snowmelt runoff estimates from this basin improved when initialized with passive microwave SWE estimates as compared to using available observational and satellite-based meteorological data alone.

Passive microwave SWE retrieval algorithms have typically relied on empirical relationships between either snow depth or SWE and frequency dependent signal scattering through the snowpack at different channels

[*Chang et al*., 1987]. An estimate of the SWE is obtained by taking the difference between the return signals at two different passive microwave frequencies: a low frequency, typically 18–19 GHz, where scattering by snow is less than at a high frequency, typically around 37 GHz, and applying a coefficient derived from radiative transfer theory. Several sources of error in microwave SWE retrievals stem from the dynamic nature of snow and the static assumptions made in the empirical formulations concerning snow properties. Studies have shown emission signatures to be affected by snow depth [*Dong et al*., 2005; *Foster et al*., 2005]. It is estimated that the signal "saturates" at 1 m depth (or approximately 250 mm SWE), above which soil emissions through the snowpack at the higher frequency microwave signal are no longer detectable [*Clifford*, 2010]. Liquid water in the snowpack is significantly more absorptive than ice at the microwave frequencies [*Mätzler*, 1987] and eliminates the brightness temperature ($T_B$) gradient used to estimate SWE [*Hallikainen et al*., 1986; *Walker and Goodison*, 1993]. Therefore, many studies avoid evaluating passive microwave data during the spring, when snow melt and rainfall can introduce error in the data. Other snowpack characteristics such as density and crystal size also affect the passive microwave signal by increasing the spectral gradient with increases in grain growth [*Foster et al*., 1999; *Hall et al*., 1986; *Josberger and Mognard*, 2002; *Durand et al*., 2011].

*Mätzler and Standley* [2000] suggested that topography of the ground has a significant impact on microwave retrievals. However, other studies found little or no evidence of error due to elevation gradients over large regions [*Dong et al*., 2005; *Vuyovich and Jacobs*, 2011]. It is possible that errors due to terrain are averaged out over large pixel areas or that in high elevation regions more significant error is caused by the saturation of the signal in deep snow. Several studies have shown a significant impact of vegetation on the passive microwave signal because the liquid water in the tree branches and leaves emits microwave radiation [*Chang et al*., 1996; *Foster et al*., 2005; *Derksen et al*., 2005]. *Vander Jagt et al*. [2013] found that in pixels with significant vegetation, the error in the passive microwave estimate was on the same order of magnitude as the actual snow depth, making the data virtually unusable. Ongoing research, which has attempted to account for these errors and to improve results regionally and seasonally, has had varied success [*Farmer et al*., 2010; *Tedesco and Narvekar*, 2010; *Mizukami and Perica*, 2012].

The NWS National Operational Hydrologic Remote Sensing Center (NOHRSC) offers a near real-time 1 $km^2$ spatially distributed estimate of SWE and other snow properties across the continental United States (CONUS) through its SNOw Data Assimilation System (SNODAS). SNODAS integrates a combination of downscaled forcing data, an energy balance snow model and assimilated observations in their daily gridded SWE product to arrive at their best estimate of the snow characteristics over the United States and to minimize error associated with any individual method [*Carroll et al*., 2006]. Though these data are also subject to errors, this product provides the only real-time spatially distributed estimate of snowpack conditions throughout the U.S. and is used operationally at several locations [e.g., *Lea and Reid*, 2006; *Schneiderman et al*., 2013]. The snow model within SNODAS has been evaluated and generally shown to provide good results at a point scale [*Rutter et al*., 2008; *Frankenstein et al*., 2008], though over a larger scale, particularly where ground observations are sparse or biased, additional error is introduced [*Molotch and Bales*, 2005; *Meromy et al*., 2013]. In the Sierra Nevada, *Rittger et al*. [2011] and *Dozier* [2011] showed that SNODAS estimates of SWE are less than reconstructed SWE values and spring runoff volumes, while *Guan et al*. [2013] found that a blended estimate of reconstruction and ground observations provided the best results. *Clow et al*. [2012] used field surveys and water balance analysis to evaluate SNODAS SWE in headwater basins in Colorado. They found good agreement in forested areas, but poor agreement in areas impacted by wind redistribution of the snowpack.

A few previous efforts to evaluate the passive microwave estimates of SWE have used the SNODAS product for comparison. *Azar et al*. [2008] evaluated the SSM/I SWE products in the Great Lakes region using the SNODAS data and found poor results using the original passive microwave algorithm. *Tedesco and Narvekar* [2010] compared monthly estimates of AMSR-E SWE to SNODAS (resampled at 25 km) over the 2004–2005 winter season, and found poor correlation when evaluating the entire U.S. They also classified the pixels by forest cover fraction and found better correlations in areas of higher forest fraction and density, which they attributed to shallow snow in the open areas.

This study aims to provide a comprehensive examination of the regional characteristics associated with satellite observations of SWE at a scale useful for water resource applications in the United States. We hypothesize that existing microwave retrieval algorithms will compare favorably to the SNODAS SWE estimates in

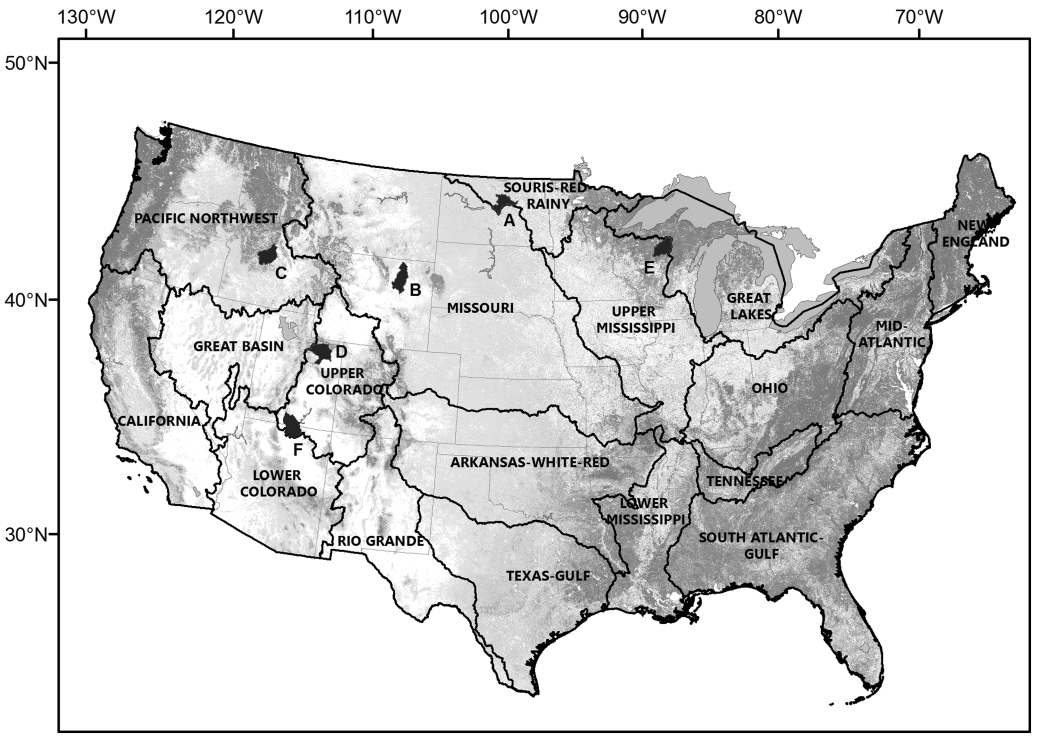


**Figure 1.** Overview map of the study region with HUC2 watersheds outlined and percentage forest cover shown. Example watersheds are shown in black and labeled.

basins which have minimal vegetation or topography and where the snow depth does not exceed a saturation threshold. To test this hypothesis, we analyzed the SWE estimates derived from two satellite sensors, AMSR-E and SSM/I, and the SNODAS daily gridded SWE by watersheds across the U.S. to evaluate the value of these snow data in hydrologic processes. Comparison at the basin scale also provides future opportunity to evaluate the SWE in conjunction with watershed runoff. There are several questions this research aims to answer:

1. In which U.S. basins do passive microwave estimates of SWE compare well to the SNODAS product as evaluated by correlation and rank-order of the peak SWE and seasonal snowpack evolution?
2. Is the level of agreement a function of forest cover, elevation or maximum SWE?
3. In basins where passive microwave SWE does not match the magnitude of SNODAS data is there a common pattern of snow accumulation and melt, year-to-year variability, or relative magnitude?

## 2. Study Area and Data

For this study, the SWE products were compared by major hydrologic regions of the continental U.S. The USGS fourth level basins, designated by an eight digit Hydrologic Unit Code (HUC), were selected for comparison. There are 2100 HUC-8 basins, with an average area of 3700 km$^2$. The elevation range within each of the HUC-8 basins was determined using the USGS 1 arc sec (approximately 30 m) national elevation data set (NED) (data available from the USGS). The Vegetation Continuous Field from the University of Maryland [*Hansen et al*., 2006] was used to estimate the percentage of forest cover by HUC. In addition, regional comparisons were made using the 18 USGS first level basins, designated by a two digit HUC, which have an average area of 434,000 km$^2$ (Figure 1).

### 2.1. Passive Microwave

Daily passive microwave SWE data were available from two sources during the period of comparison; the Special Sensor Microwave/Imager (SSM/I) and the Advanced Microwave Scanning Radiometer-Earth Observing System (AMSR-E). The SSM/I sensor was launched in 1987 on board the Defense Meteorological Satellite

Program (DMSP) satellites. These data are available near real-time and have the advantage of a long historical record. SWE estimates are derived from the SSM/I brightness temperatures measured at wavelengths 19 and 37 GHz, and have a spatial resolution of 69 × 43 km (19.4 GHz) and 37 × 29 km [*Armstrong et al*., 1995]. SSM/I data were processed using the Chang algorithm:

$$\mathrm{SWE} = c(T_{B,19} - T_{B,37}) \tag{1}$$

where SWE is in mm; $T_B$ is the temperature brightness at different channels (K); and $c$ is typically given as 4.8 mm/K and acquired from the National Snow and Ice Data Center (M. J. Brodzik, NSIDC, personal communication, 2012).

AMSR-E was launched on NASA's Aqua satellite in 2002 and calculates SWE based on brightness temperatures measured at wavelengths 19.7 and 36.5 GHz, with a spatial resolution of 28 × 16 km (19.7 GHz) and 14 × 8 km (36.5 GHz) [*Kelly*, 2009]. For this study, AMSR-E data were acquired from NSIDC (http://nsidc.org/data/AE_DySno), which was processed using the *Kelly* [2009] algorithm. That process uses additional bands at 10 and 89 GHz to aid in the detection of deep and shallow snow, respectively, and the algorithm accounts for the forest fraction of the underlying ground,

$$SD = ff\left[p1\frac{(T_{B,V18} - T_{B,V36})}{(1 - b * fd)}\right] + (1 - ff)\left[p1\left(T_{B,V10} - T_{B,V36}\right) + p2\left(T_{B,V10} - T_{B,V18}\right)\right] \tag{2}$$

where $SD$ is snow depth (cm), $ff$ is forest fraction, $fd$ is forest density, $b$ is an optimized coefficient found to be 0.6, and $p1$ and $p2$ are dynamic coefficients calculated as the difference in polarization at channels 36 and 18, respectively. Snow depths are then converted to SWE using seasonal density estimates for different snow classes based on *Sturm et al*. [1995].

SSM/I and AMSR-E global SWE products are produced using these algorithms and available twice daily; ascending passes which occur in the afternoon and descending passes which occur in the early morning. For this study, only descending SWE data were used to reduce the potential wet snow impacts in the afternoon. A gap in the satellite swath coverage can occur every 3–4 days, depending on the latitude of the region. This study uses the products' EASE-grid projection at a 625 km$^2$ (25 km × 25 km) resolution.

### 2.2. SNODAS

The NOAA's SNODAS combines data from various sources—ground observations, airborne and satellite estimates—with model results, to arrive at a 1 km$^2$ spatially distributed estimate of snow cover and SWE [*Carroll et al*., 2006]. Their procedure follows three main steps; ingest and downscale model weather data, simulate snow cover using a physically based energy balance model, and assimilate snow observations to adjust model results. Forcing data come from the Rapid Update Cycle 2 (RUC2) Numerical Weather Prediction (NWP) model output and is downscaled from 13 to 1 km resolution using a digital elevation model. The snow model is an energy and mass-balance, multilayer model based on SNTHERM.89 [*Jordan*, 1990]. Assimilated observations are acquired from state and federal automated ground observations, snow surveys, and gamma flights as well as satellite-based snow extent information. SNODAS data are available through NSIDC from 1 October 2003 to the present (http://nsidc.org/data/G02158).

## 3. Methods

Gridded daily SWE data from the two passive microwave sensors and SNODAS were obtained for eight water years, 2004–2011, when all three data sets were available. For each of the AMSR-E, SSM/I, and the SNODAS SWE data sets, the gridded data were aggregated by HUC-8 to produce a daily time series of average-basin SWE. To avoid large gaps along the watershed boundaries, the passive microwave data were resampled to 1 km$^2$ grid cells using the nearest neighbor method which assigns the same value to the pixel as the data layer in that location without any interpolation. AMSR-E pixels near large water bodies are flagged within the SWE product and no SWE value is given; therefore only watersheds with no missing data were used in the comparison. Weekly SWE time series were developed for each HUC-8 using the maximum weekly values in order to accommodate the satellite overpass cycle which results in some days without satellite observations. Annual maximum SWE values by HUC were extracted from the weekly time series for

each of the eight water years. The results are summarized regionally by aggregating results to the 18 two digit HUCs.

The average, maximum, minimum, and standard deviation of the daily SWE was determined for each HUC over the periods of interest. The differences in average annual maximum SWE were calculated between the SNODAS and passive microwave data sets to determine the difference in relative magnitude of the estimates. The correlation coefficients between microwave SWE and SNODAS estimates for the annual and weekly time series were also calculated. Differences between SNODAS and the microwave values of annual maximum SWE values were identified using the Spearman's rank-order test. Spearman's rank-order test determines whether two independent groups are from the same population [*Helsel and Hirsch*, 2002]. To evaluate spatial variability within the HUC-8s, the SNODAS data were aggregated to the 25 km by 25 km pixel scale using a pixel average. The standard deviation of SNODAS SWE with each HUC-8 was then calculated similarly to the passive microwave data in order to compare the data at the same coarse resolution.

Weekly SWE results were compared using the Nash-Sutcliffe model efficiency index [*Nash and Sutcliffe*, 1970], which measures the fit between predicted and observed values as:

$$Efficiency = 1 - \left( \frac{\sum_{i=1}^{N} (SWE_{obs,i} - SWE_{sat,i})^2}{\sum_{i=1}^{N} (SWE_{obs,i} - \overline{SWE}_{obs,i})^2} \right) \quad (3)$$

where $N$ is the number of weeks during the simulation period, $SWE_{obs,i}$ is the SNODAS $i$th weekly SWE, $SWE_{sat,i}$ is the $i$th weekly SWE value estimated from the AMSR-E or SSM/I data set, and $\overline{SWE}_{obs,i}$ is the mean weekly SNODAS SWE value for the simulation period. This metric characterizes the joint evolution of passive microwave and modeled SWE over the entire winter rather than just the peak SWE. While the SNODAS data were used as the observational data set in this measure, it is important to note that the model itself has errors and is not considered ground truth. The efficiency will approach unity if each SNODAS weekly SWE value matches the remotely sensed weekly SWE value.

The effects of saturation depth, elevation range, and forest cover on SWE estimates were evaluated by calculating correlations between SNODAS and passive microwave average maximum SWE for each HUC-8 by category. The saturation depth was assessed by comparing passive microwave to SNODAS at increasing amounts of average maximum annual SWE. The elevation range was evaluated to address the impact of topography on SWE estimates, and was calculated for each HUC-8 as the difference in maximum and minimum elevation in each basin. Correlations between the passive microwave and SNODAS SWE were determined for eight elevation range categories. Correlations were also determined for SWE estimates by 10% increments in total basin forest fraction.

## 4. Results and Discussion

### 4.1. Overall Performance

The agreement between average annual maximum SWE for the SNODAS product and the AMSR-E and SSM/I passive microwave data varies widely across regions of the United States (Figure 2). As anticipated, the passive microwave data underestimate the SWE for those regions that experience significant annual snowpacks including the Rocky Mountains, the Pacific Mountain Range, and Northern New England. The saturation effect appears to be evident when SWE from SNODAS exceeds 150–200 mm. For the western ranges, the snowpacks' SWE frequently exceeds 500 mm based on the SNODAS product. AMSR-E is able to identify the location of those ranges as having relatively deeper snow, but greatly underestimates the SWE magnitude. SSM/I entirely misses many of these deep snow features. This result broadens *Andreadis and Lettenmaier*'s [2006] finding that passive microwave data are problematic when snowpacks were deeper than 240 mm for Snake River basin in the western U.S. A new finding is that this disagreement is also broadly evident for those regions in the Northeast in which SWE exceeds 240 mm. In the Northeast region, the AMSR-E data show better agreement to the SNODAS product than SSM/I which reports little to no snow. This result extends the modest agreement found previously in the Northeast region, which only analyzed a single, historic storm in the Middle Atlantic [*Foster et al.*, 2012].

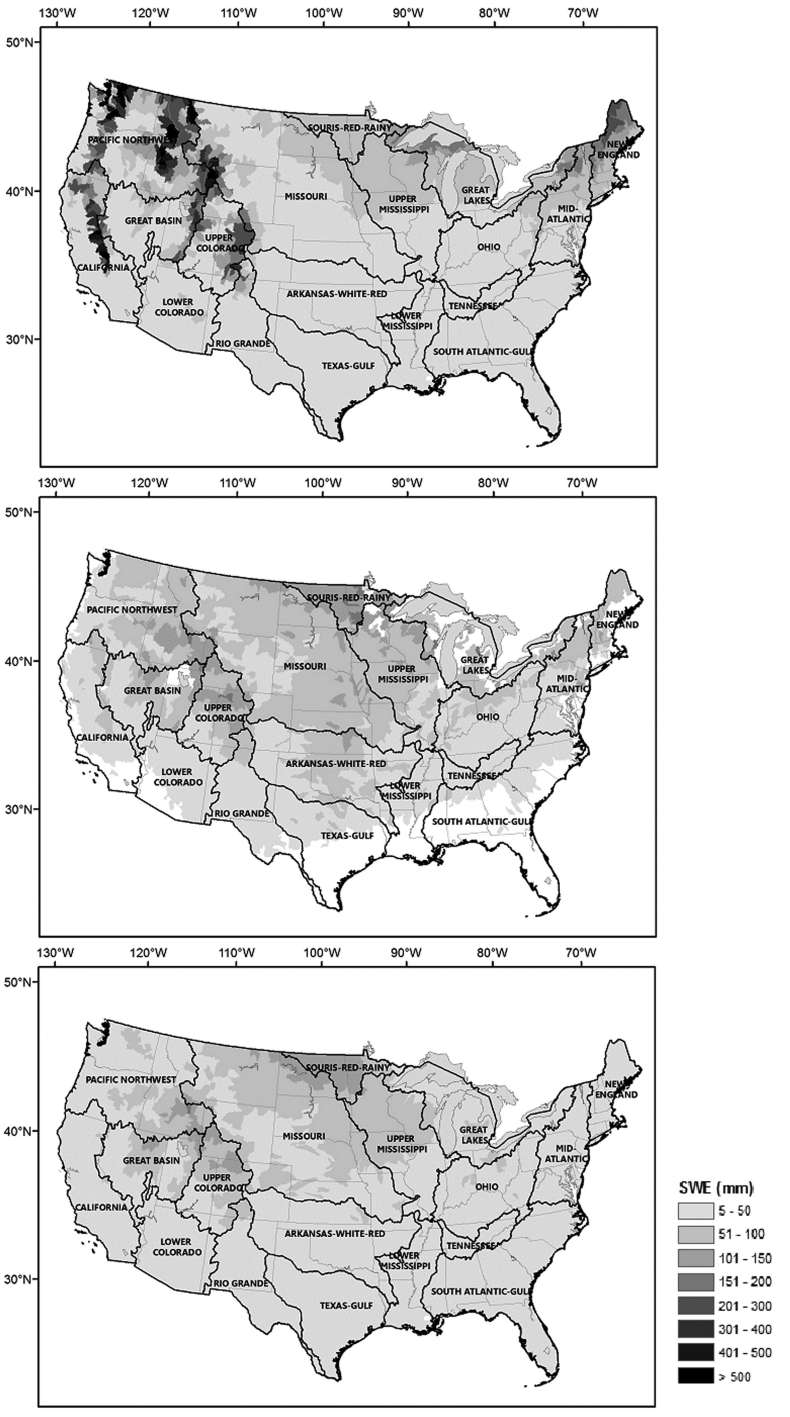


**Figure 2.** Average maximum annual SWE by HUC-8 for (a) SNODAS, (b) AMSR-E, and (c) SSM/I.

Interestingly, the passive microwave data are not consistently less than the SNODAS product. In the Plains regions and the southeastern portions of the U.S., microwave SWE products indicated greater maximum annual SWE values than SNODAS (Figure 3). This is a region with relatively few observational data available to correct the SNODAS model. Because both microwave products have deeper snowpacks in the northern Plains region, the actual SWE may be underestimated by SNODAS. This theory is supported by previous work by *Josberger et al*. [1998] who suggest that the northern Great Plains region is well suited for estimation of SWE from microwave observations. In this same region, *Chang et al*. [2005] showed that the midwinter microwave estimates of snow depth had a calculated error of 88 mm, but also pointed to the strong heterogeneity of snow depth across the region which made validation quite difficult.

In the southern Plains, the SNODAS SWE values are consistent with the SSM/I SWE values but overestimated by the AMSR-E observations. The AMSR-E data appear to be biased high in shallow snow regions, particularly in the southern Plains. A nominal 50 mm snow depth is applied when the AMSR-E algorithm detects shallow snow [*Kelly*, 2009]. *Armstrong and Brodzik* [2002] found that inclusion of the shallow snow detection algorithm led to overestimation of SWE in some regions. *Daly et al*. [2012] similarly found early season SWE detection by AMSR-E in Afghanistan was not supported by multispectral imagery of snow extent.

In regions with significant SWE biases, the relative SWE magnitude across years may still be robust and able to provide insight for water resource management. Parametric and nonparametric methods were used to

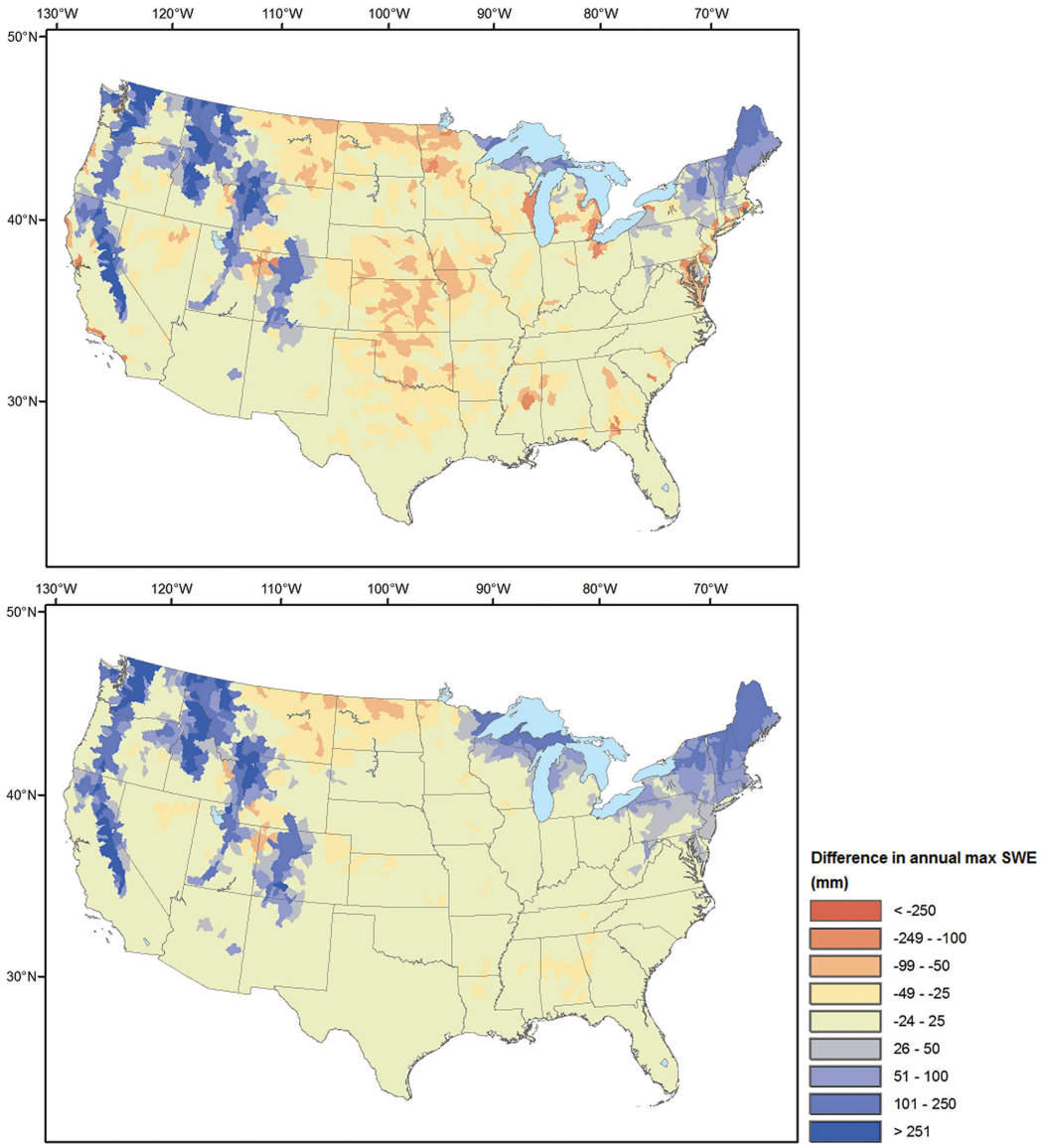


**Figure 3.** Difference in average maximum annual SWE by HUC-8 for (a) SNODAS-AMSR-E and (b) SNODAS-SSM/I.

characterize the correlation of the annual maximum time series between the SNODAS data and each of the passive microwave data sets (Table 1). The strongest and significant correlations between SNODAS and the AMSR-E and SSM/I products occur in the northern Plains region (Upper Mississippi and Missouri) and in the southern Rocky Mountains (Lower Colorado). SNODAS and the AMSR-E SWE estimates also show good agreement along the Great Lakes region (Ohio), while the SSM/I data are well correlated with SNODAS in the Pennsylvania region (Mid-Atlantic). For many of the regions, there is not a significant correlation suggesting that either passive microwave or SNODAS SWE estimates are not accurate in that region or that the two methods provide different information.

Based on the Spearman's rank-order statistic, AMSR-E and SSM/I are not able to capture the relative magnitude of the annual peak SWE for the Upper Colorado, New England, and the Pacific Northwest; the three HUC-2 regions having SWE values higher than 80 mm. The passive microwave data do not seem to capture the relative magnitude of the annual peak SWE when it underestimates the total SWE. Limited agreement is also evident for the four HUCs, Texas-Gulf, South Atlantic-Gulf, Lower Mississippi, and Tennessee, having the lowest peak snow values, which could be due to limited observations available impacting the SNODAS results or SWE values below a threshold level for detection by passive microwave.

**Table 1.** HUC-2 Data and Average Annual Maximum SWE Statistics ($N = 8$)[a]

| HUC2 | Region | Area ($\times 10^3$ km$^2$) | Forest Fraction | Elevation Range (m) | SNODAS Average Annual Maximum SWE (mm) | AMSR-E Average Annual Maximum SWE (mm) | SSM/I Average Annual Maximum SWE (mm) | SNODAS and AMSR-E $R^2$ | SNODAS and SSM/I $R^2$ | SNODAS and AMSR-E Sp. Rho | SNODAS and SSM/I Sp. Rho |
|---|---|---|---|---|---|---|---|---|---|---|---|
| 1 | New England Region | 158 | 0.81 | 1856 | 118.3 | 30.1 | 10.4 | 0.26 | 0.15 | 0.40 | 0.24 |
| 2 | Mid-Atlantic Region | 288 | 0.73 | 1511 | 45.9 | 23.8 | 11.9 | 0.35 | **0.79** | **0.86** | **0.95** |
| 3 | South Atlantic-Gulf Region | 698 | 0.55 | 1765 | 4.3 | 2.7 | 5.9 | 0.08 | 0.14 | 0.26 | −0.02 |
| 4 | Great Lakes Region | 303 | 0.42 | 1200 | 70.8 | 32.6 | 25.4 | **0.62** | 0.24 | **0.83** | 0.24 |
| 5 | Ohio Region | 422 | 0.67 | 1591 | 28.2 | 21.2 | 13.0 | 0.37 | **0.63** | 0.48 | 0.69 |
| 6 | Tennessee Region | 106 | 0.90 | 1849 | 11.4 | 10.6 | 13.8 | 0.01 | 0.02 | 0.67 | 0.48 |
| 7 | Upper Mississippi Region | 492 | 0.10 | 593 | 46.9 | 42.0 | 43.0 | **0.63** | 0.75 | **0.76** | 0.83 |
| 8 | Lower Mississippi Region | 262 | 0.45 | 822 | 6.8 | 8.7 | 8.4 | **0.47** | 0.22 | 0.60 | 0.38 |
| 9 | Souris-Red-Rainy Region | 154 | 0.14 | 521 | 76.6 | 95.4 | 93.1 | 0.24 | **0.53** | 0.48 | 0.52 |
| 10 | Missouri Region | 1324 | 0.12 | 4106 | 39.0 | 42.6 | 39.5 | **0.66** | **0.65** | 0.62 | 0.57 |
| 11 | Arkansas-White-Red Region | 642 | 0.25 | 4233 | 16.2 | 21.4 | 13.4 | 0.10 | **0.67** | 0.43 | 0.76 |
| 12 | Texas-Gulf Region | 464 | 0.12 | 1449 | 4.2 | 8.2 | 5.6 | 0.11 | 0.13 | 0.19 | 0.60 |
| 13 | Rio Grande Region | 344 | 0.09 | 4096 | 16.4 | 15.1 | 7.8 | 0.13 | **0.64** | 0.17 | **0.74** |
| 14 | Upper Colorado Region | 293 | 0.27 | 3204 | 81.4 | 62.7 | 53.1 | 0.41 | 0.14 | 0.57 | 0.38 |
| 15 | Lower Colorado Region | 363 | 0.11 | 3687 | 14.5 | 13.3 | 7.2 | **0.65** | **0.97** | **0.76** | **0.90** |
| 16 | Great Basin Region | 368 | 0.09 | 3536 | 53.0 | 47.0 | 36.3 | 0.09 | 0.03 | 0.45 | −0.02 |
| 17 | Pacific Northwest Region | 710 | 0.49 | 4403 | 141.4 | 43.4 | 30.5 | **0.54** | 0.30 | 0.62 | 0.57 |
| 18 | California Region | 417 | 0.31 | 4350 | 64.7 | 13.2 | 7.6 | 0.09 | 0.01 | 0.60 | 0.26 |

[a]Bold indicates statistically significant values where critical values are $R^2$ equal 0.46 and Spearman's ranked correlation coefficient equal 0.738.

The standard deviation of estimated SWE within each HUC-8 watershed was calculated daily over the period of record to assess the spatial variability of estimates within each basin. SNODAS data were aggregated to the microwave EASE-GRID pixel size in order to match the microwave scale. Figure 4 shows an example of the results on 1 February 2011. There is greater variability within the deep snow regions along the Pacific mountains and the Rocky Mountains for SNODAS. The AMSR-E data have greater variability than the SSM/I data, particularly in the New England region where the SSM/I data shows none. In the Plains basins, the three data sources compare favorably in most years with the exception of the southern Plains region (e.g., Texas/Oklahoma). In this region, the relatively high variability of the passive microwave data, particularly AMSR-E, result from positive SWE values in pixels where none is likely to exist.

The weekly SWE from the microwave products was compared to the SNODAS product using the Nash-Sutcliffe efficiency statistic (Table 2). Strong weekly results are evident for the regions that performed well for interannual variability, e.g., the northern Plains and southern Rockies. Other regions showed promise, such as the Upper Colorado basin, despite having maximum SWE values that might exceed the passive microwave threshold for detection. The passive microwave observations appear to be able to capture the timing of snow accumulation and melt. A region that stands out for the disagreement between SNODAS and passive microwave in the weekly SWE analysis is the central Plains. This region does not have significant vegetation or snow depths that would be expected to impact the microwave signal. It is possible that the SNODAS SWE estimates suffer from lack of observations, though additional work is required to understand the differences seen in this area.

Overall, passive microwave derived SWE estimates appear to perform the best when the typical HUC-2 annual maximum SWE values are between 15 and 50 mm. Within this range, there is good correlation for year to year differences and value in the weekly observations. The AMSR-E observations provide SWE estimates that have limited bias as compared to the SNODAS data. At modestly higher SWE values, between 50 and 80 mm, there is a mixture of results with the passive microwave having greater success at matching the snowpack's temporal evolution as compared to the magnitude of the annual maximums.

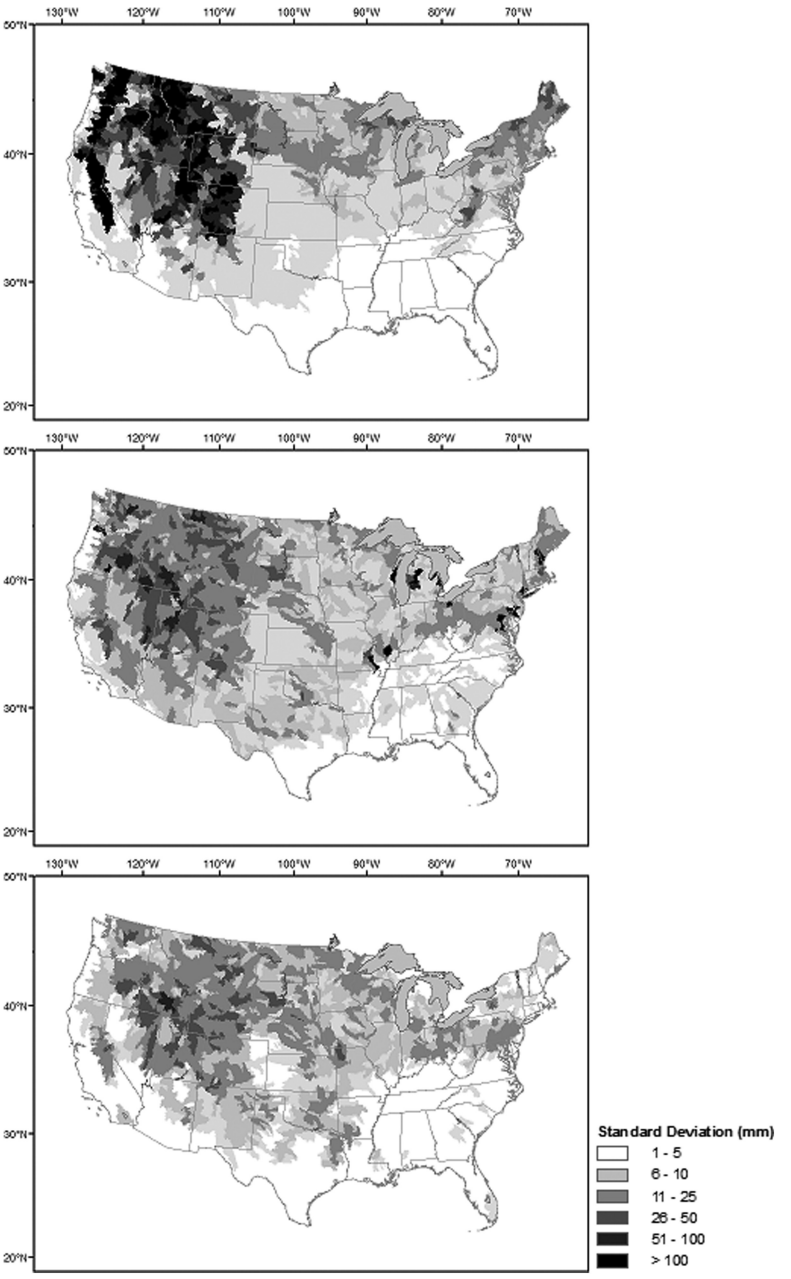


**Figure 4.** Standard deviation of SWE by HUC-8 on 1 February 2011 for (a) SNODAS, (b) AMSR-E, and (c) SSM/I.

### 4.2. Effect of Physical Characteristics

The SWE data were analyzed by forest cover, saturation depth, and elevation range to determine what impact these factors had on the results. For forest cover, the strongest correlations occur in HUCs with 20% forest coverage or less, with generally poorer correlations occurring with more vegetation (Figure 5). The exceptions are along the East coast, where AMSR-E shows good correlations ($>$0.5) with SNODAS data in watersheds along the eastern side of the Appalachians, North Carolina up through Virginia, and SSM/I doing well in central Pennsylvania and New York. In the heavily forested regions of New England and around the Great Lakes, both AMSR-E and SSM/I underestimate the maximum SWE values, though AMSR-E performs better than SSM/I. It is expected that these regional differences between the two microwave data sets' results are a function of the retrieval algorithms used. While AMSR-E, unlike SSM/I, accounts for forest fraction in the current algorithm, vegetation type is not included. *Azar et al*. [2008] were able to improve the SSM/I results in the Great Lakes region by developing an algorithm that uses a Normalized Difference Vegetation Index (NDVI) to classify the mixed use forest in the region.

Passive microwave estimates of SWE are best correlated with SNODAS data in regions where the maximum annual SWE values are relatively low and agreement decreases as the SWE increases (Figure 6). In watersheds with an annual maximum SWE less than 100 mm, the SSM/I SWE product is better correlated with SNODAS than AMSR-E. Above 100 mm, AMSR-E has consistently better agreement with SNODAS than SSM/I, though both correlations decrease with increasing snow depth.

More than half of the eight digit HUCs, or 56% of the total area in the conterminous U.S., have less than 20% forest coverage. For the regions with less than 200 mm annual maximum SNODAS SWE and less than 20%

**Table 2.** HUC-2 Weekly Statistics for Winter Months: October–April ($N = 242$)

| HUC2 | Region | SNODAS Average Weekly SWE (mm) | AMSR-E Average Weekly SWE (mm) | SSM/I Average Weekly SWE (mm) | SNODAS and AMSR-E Weekly SWE $R^2$ | SNODAS and SSM/I Weekly SWE $R^2$ | SNODAS and AMSR-E Weekly Nash-Sutcliffe | SNODAS and SSM/I Weekly Nash-Sutcliffe |
|---|---|---|---|---|---|---|---|---|
| 1 | New England Region | 47.8 | 11.3 | 2.4 | 0.61 | 0.33 | −0.28 | −0.85 |
| 2 | Mid-Atlantic Region | 13.0 | 7.0 | 2.0 | 0.69 | 0.43 | 0.43 | −0.30 |
| 3 | South Atlantic-Gulf Region | 0.4 | 0.3 | 0.7 | 0.11 | 0.00 | 0.08 | −1.44 |
| 4 | Great Lakes Region | 26.8 | 10.4 | 5.4 | 0.71 | 0.65 | 0.10 | −0.36 |
| 5 | Ohio Region | 5.5 | 4.0 | 1.9 | 0.74 | 0.50 | 0.68 | 0.22 |
| 6 | Tennessee Region | 1.6 | 1.3 | 1.0 | 0.14 | 0.01 | 0.01 | −0.38 |
| 7 | Upper Mississippi Region | 15.6 | 14.9 | 10.9 | 0.78 | 0.74 | 0.77 | 0.67 |
| 8 | Lower Mississippi Region | 0.6 | 0.9 | 0.6 | 0.04 | 0.00 | −0.34 | −0.59 |
| 9 | Souris-Red-Rainy Region | 31.1 | 32.5 | 30.7 | 0.66 | 0.75 | 0.62 | 0.69 |
| 10 | Missouri Region | 17.5 | 16.9 | 13.7 | 0.73 | 0.76 | 0.70 | 0.67 |
| 11 | Arkansas-White-Red Region | 3.2 | 4.0 | 2.2 | 0.48 | 0.62 | 0.30 | 0.58 |
| 12 | Texas-Gulf Region | 0.4 | 0.7 | 0.3 | 0.23 | 0.07 | −0.48 | −0.21 |
| 13 | Rio Grande Region | 7.2 | 4.5 | 2.2 | 0.44 | 0.64 | 0.27 | −0.10 |
| 14 | Upper Colorado Region | 42.4 | 27.2 | 20.9 | 0.67 | 0.59 | 0.43 | 0.14 |
| 15 | Lower Colorado Region | 4.0 | 3.6 | 1.2 | 0.63 | 0.80 | 0.62 | 0.37 |
| 16 | Great Basin Region | 24.3 | 19.8 | 12.0 | 0.60 | 0.57 | 0.55 | 0.20 |
| 17 | Pacific Northwest Region | 73.1 | 19.6 | 13.5 | 0.55 | 0.55 | −0.51 | −0.78 |
| 18 | California Region | 27.3 | 5.3 | 2.9 | 0.38 | 0.45 | −0.58 | −0.79 |

forest cover, the $R^2$ values between SNODAS and AMSR-E, and SNODAS and SSM/I average annual maximum SWE are 0.48 and 0.66, respectively. Figure 7 shows the $R^2$ values between SNODAS and the passive microwave weekly SWE for each HUC-8 during the winter months (October–April). Basins with the best agreement tend to fall outside the areas with greater than 20% forest coverage and greater than 200 mm annual maximum SNODAS SWE, though several basins with weekly correlations greater than 0.5 do reside in those areas.

The analysis of SWE estimates with terrain does not show a consistent relationship between elevation range and correlation of the data. Once basins with greater than 20% forest coverage and a greater than 200 mm average maximum SNODAS SWE were removed, good correlations occur between SNODAS and the passive microwave data despite large changes in topography. *Dong et al*. [2005] investigated the impacts of topographic roughness on SWE estimates at over 3000 observing stations in Canada, and found no significant impact compared to the effects of deep snow and nearby water bodies. *Tong et al*. [2010] found that while algorithms performed better in complex terrain when only SWE values less than 250–400 mm were considered, the accuracy was still insufficient at a point comparison. At a large watershed scale, the effects of topography are expected to average out, having a minimal effect on error compared to vegetation and snow depth.

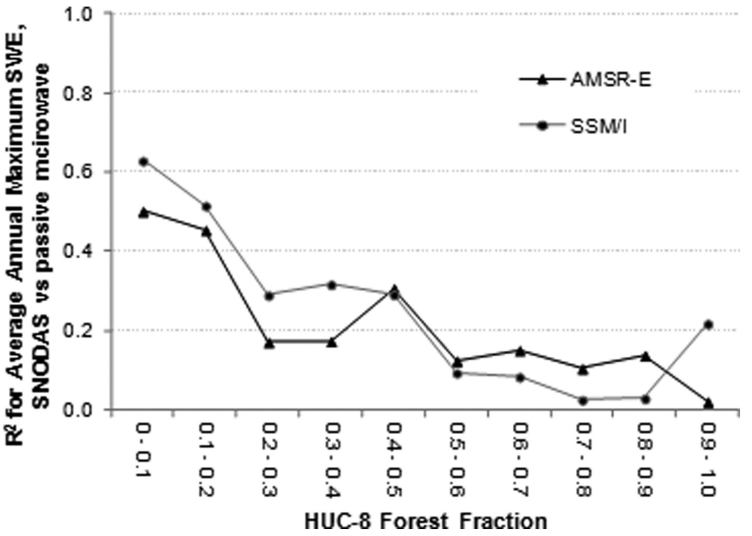


**Figure 5.** $R^2$ of average annual maximum SWE in HUC-8s by forest fraction.

Times series of SWE data in basins from six different regions demonstrate typical regional differences in the weekly comparison (Figure 8). Characteristics of each of the basins and statistical results of the comparison of passive microwave SWE with SNODAS data are given in Table 3. The Sheyenne Basin (A) is in the northern Plains region where all three data sets compare very well. In this region, the evolution and magnitude are typically similar with correlations between SNODAS and passive

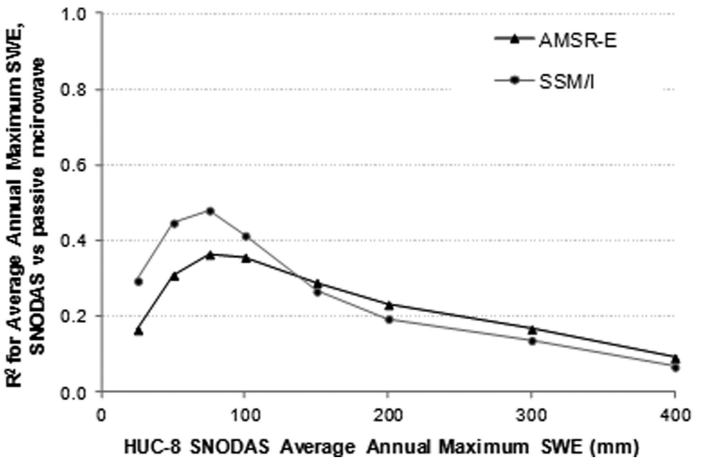


**Figure 6.** $R^2$ of average annual maximum SWE in HUC-8s for increasing categories of SNODAS SWE.

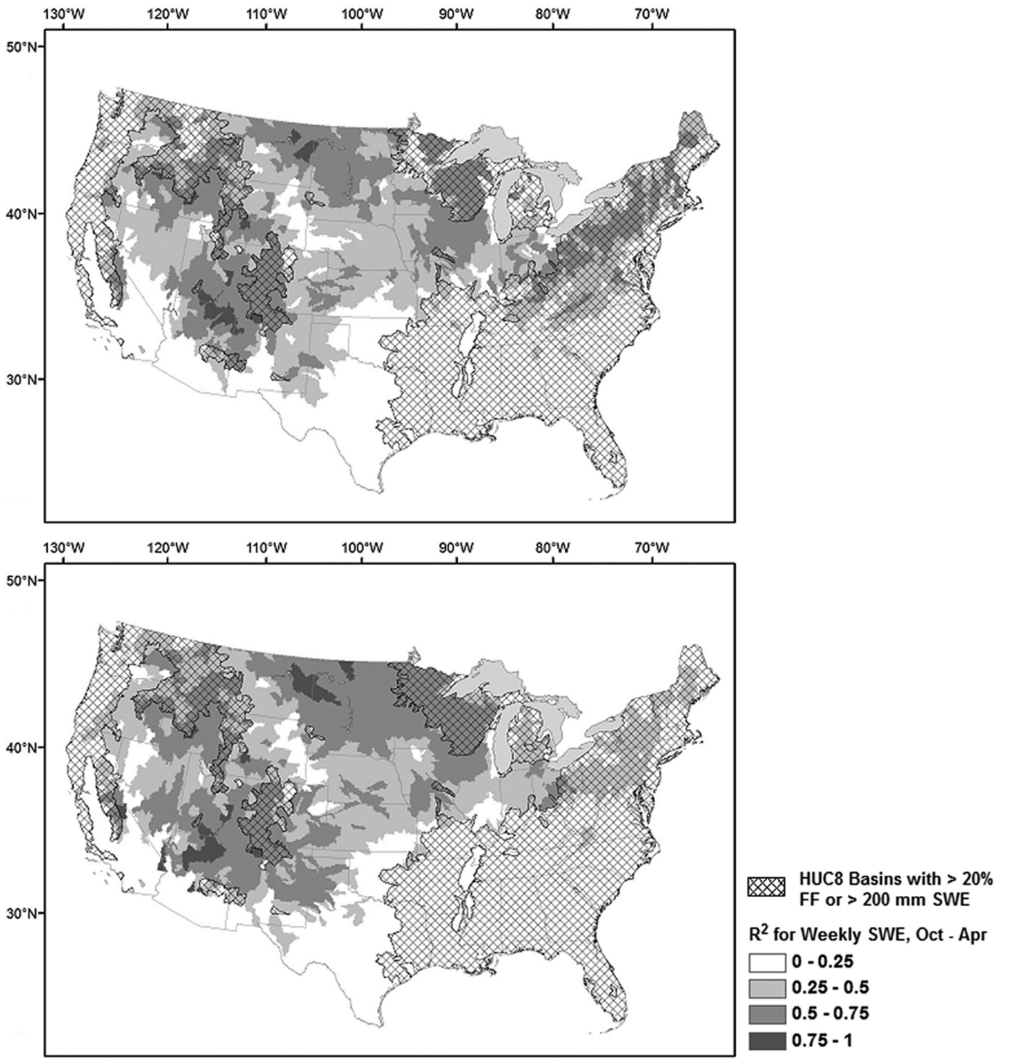


**Figure 7.** $R^2$ of weekly winter SWE, October–April, by HUC-8 for (a) SNODAS and AMSR-E, (b) SNODAS and SSM/I; hatched area shows HUCs with greater than 20% forest coverage or an average maximum annual SNODAS SWE greater than 200 mm.

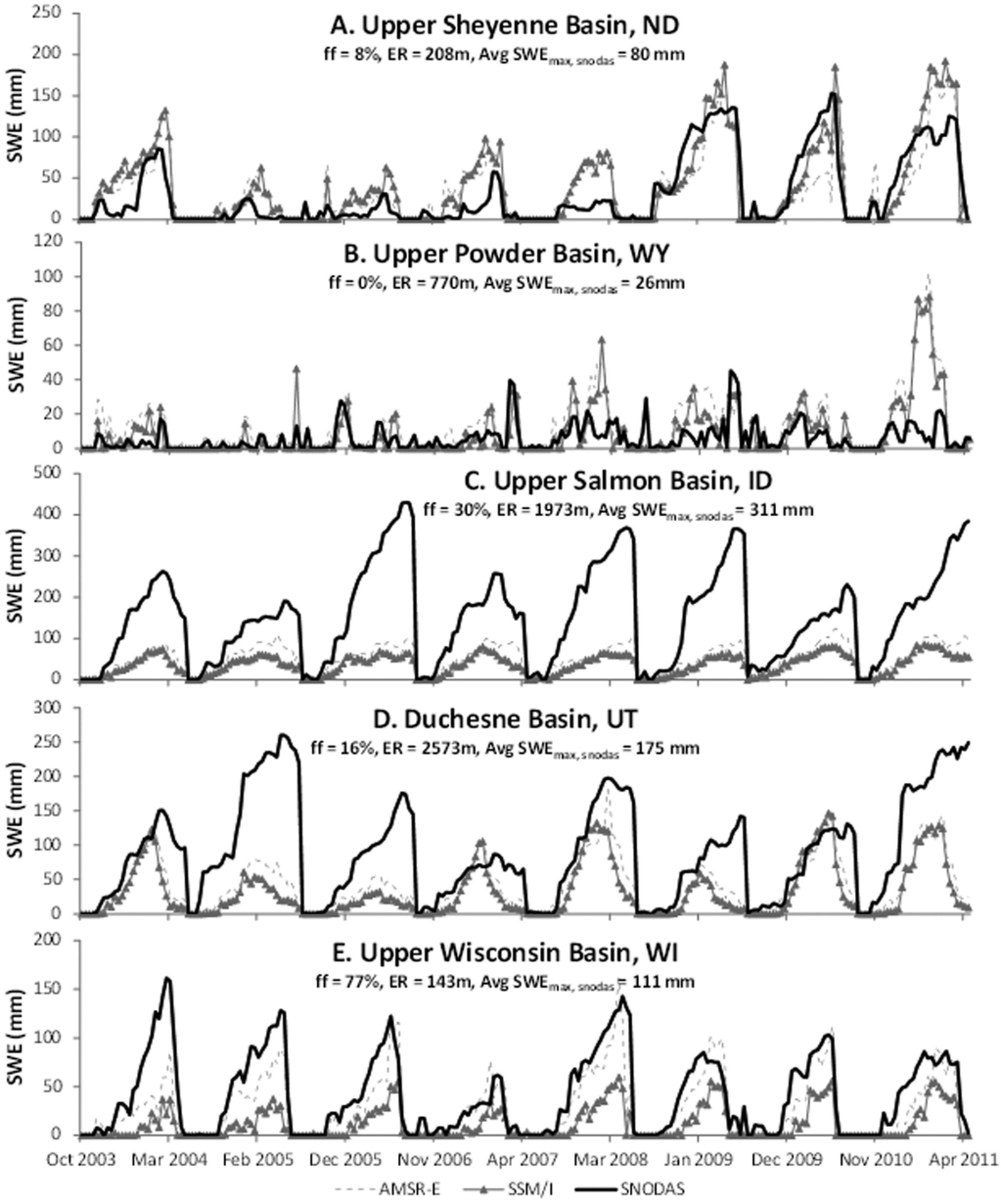


**Figure 8.** Example time series of average-basin SWE in different regions (shown in Figure 1), with high and low forest fractions (ff), elevation ranges (ER), and average maximum annual SWE (based on SNODAS).

microwave of 0.55 and 0.68 for AMSR-E and SSM/I, respectively, and Nash-Sutcliffe efficiencies between SNODAS and passive microwave data of 0.48 and 0.52 for AMSR-E and SSM/I, respectively. The Upper Powder Basin (B) is in the Central Plains region where the agreement is not as strong. The basin has a modest snowpack that is tracked by all data sets, but the strongly negative Nash-Sutcliffe efficiencies show the lack of agreement between the time series. The Upper Salmon Basin (C) in the Pacific Northwest region has considerable vegetation and deep annual snowpacks. The passive microwave follows a similar accumulation and ablation trend, and has a correlation of 0.6 to the SNODAS data. However, the microwave SWE is much lower than the SNODAS SWE, even for relatively shallow snowpacks. The Duschene Basin (D) in the Upper Colorado region also receives deep snowpack but has a forest fraction of less than 20%. In lighter snow years, the passive microwave is similar in magnitude to the SNODAS SWE, but in heavier snow years the microwave data are much less, resulting in an overall negative efficiency measure. The Upper Wisconsin Basin (E) near the Great Lakes region does not experience deep snow, but is significantly forest covered. As

**Table 3.** Weekly Statistics, For Example, HUC-8 Time Series

| HUC8 | Basin | Forest Cover (%) | Elevation Range (m) | Maximum SWE (mm) | SNODAS and AMSR-E $R^2$ | SNODAS and SSM/I $R^2$ | SNODAS and AMSR-E Nash-Sutcliffe | SNODAS and SSM/I Nash-Sutcliffe |
|---|---|---|---|---|---|---|---|---|
| 9020202 | UPPER SHEYENNE, ND (Northern Plains) | 8 | 208 | 79.5 | 0.55 | 0.68 | 0.48 | 0.52 |
| 10090202 | UPPER POWDER, WY (Central Plains) | 0 | 770 | 26.0 | 0.19 | 0.21 | −3.12 | −2.22 |
| 17060201 | UPPER SALMON, ID (Northern Rockies) | 30 | 1973 | 311.5 | 0.64 | 0.62 | −0.38 | −0.71 |
| 14060003 | DUCHESNE, UT (Central Rockies) | 16 | 2573 | 174.8 | 0.43 | 0.26 | −0.03 | −0.33 |
| 7070001 | UPPER WISCONSIN, WI (Great Lakes) | 77 | 143 | 111.4 | 0.70 | 0.61 | 0.59 | −0.04 |
| 14070006 | LOWER LAKE POWELL, AZ, UT (Southern Rockies) | 0 | 2169 | 14.3 | 0.88 | 0.87 | 0.86 | 0.74 |

compared to the other four watersheds, a difference between AMSR-E and SSM/I SWE estimates is evident with AMSR-E having a Nash-Sutcliffe efficiency of 0.59 in comparison with SNODAS, while SSM/I has an efficiency in −0.04. The Lower Lake Powell Basin (F) is in the Southern Rockies region with a large elevation range, minimal vegetation, and a modest annual snowpack. Strong agreement between SNODAS and the passive microwave SWE is shown by correlations of 0.88 and 0.87 and Nash-Sutcliffe efficiencies of 0.86 and 0.74 for AMSR-E and SSM/I, respectively.

Overall, this study supports many of the findings from the earlier studies [*Dong et al*., 2005; *Vander Jagt et al*., 2013]. The SNODAS and microwave data agree in relatively flat, nonforested areas where previous studies showed promising microwave results [*Derksen et al*., 2003; *Mote et al*., 2003; *Chang et al*., 2005] and also in mountainous, nonforested regions [*Tait*, 1998; *Vuyovich and Jacobs*, 2011]. Unlike *Mätzler and Standley* [2000], this study did not find that large elevation gradients have significant impact on the passive microwave SWE estimate as compared to SNODAS SWE. *Tedesco and Narvekar* [2010] reported the highest correlations between SNODAS and AMSR-E SWE occurred in pixels with 0.3–0.4 forest fraction, whereas we found the best agreement in basins with a forest fraction of 0.2 or less. This clearly limits the regions for which microwave observations have values. Thus, inclusion of vegetation information beyond forest fraction in the retrieval algorithm (e.g., NDVI) [*Azar et al*., 2008] may expand the region for which microwave observations provide value. The thresholds are also evident for microwave SWE when snow is too deep—here we found an upper maximum of 200 mm, which is intermediate between *Clifford*'s [2010] 250 mm and *Tedesco and Narvekar*'s [2010] 90 mm. Furthermore, while there are limited studies on shallow snowpacks, our finding that the algorithm differences between AMSR-E and SSM/I challenge the quantification of watershed scale SWE estimates in southern regions is supported by *Daly et al*.'s [2012] findings from their work in Afghanistan.

## 5. Conclusion

In this study, we compared SWE estimates from AMSR-E and SSM/I passive microwave satellite sensors to the SNODAS gridded SWE product for 2100 watersheds in the U.S. No previous research has evaluated the microwave products over time at this hydrologic scale, and this provided several interesting insights. Regional differences between the AMSR-E and SSM/I point to the need to better understand the algorithms' detection of SWE in both heavily forested basins and basins with shallow annual snow. Current use of forest fraction to characterize the land in the AMSR-E algorithm seems to improve results. A more robust algorithm which includes various vegetation types may improve results further.

A comparison of the standard deviation of SWE within each HUC-8 basin showed that in areas where the passive microwave signal is impacted by deep snow and vegetation, the spatial variation also suffers. This suggests that methods to improve the microwave estimates will likely require ancillary data to determine the spatial distribution of SWE. Further research in this topic will enhance our understanding of how spatial variability within a microwave pixel is established. For instance, additional analysis of the southern plains is needed to determine if the shallow snow algorithm or some other physical process is causing AMSR-E data to overestimate SWE in this region.

Results show large areas where the passive microwave retrievals perform well compared to the SNODAS data, particularly in the northern Great Plains and southern Rocky Mountain regions. The best correlations are associated with basins in which maximum annual SWE is less than 200 mm, and forest fraction is less than 20%. While this excludes many regions of the country where snow is a significant source of water, it increases confidence in results for characteristically similar regions around the world. In the central Plains region, disagreement between SNODAS and passive microwave SWE will be the focus of future research to better understand the factors impacting the results.

In watersheds with maximum annual SWE values greater than 200 mm, poor correlations between the passive microwave data and SNODAS indicated that the relative magnitude of maximum SWE from year-to-year was not captured. However, the overall temporal pattern of accumulation and ablation did show good agreement in many of these regions, which may provide useful hydrologic information as to the snow season length and melt timing. This analysis provides a foundation for future research assessing the SWE estimates in relation to runoff from these basins.

**Acknowledgments**

This work was supported by a NASA EPSCoR grant NNX11AQ34A, the University of New Hampshire and the U.S. Army Engineer Research and Development Center's Cold Regions Research and Engineering Laboratory. We are grateful to Jeff Neihaus for his assistance in obtaining archived SNODAS data. We would like to thank Jeff Dozier, the associate editor, and two anonymous reviewers for their valuable feedback. All data used in this study are freely available and can be obtained by contacting the corresponding author.

## References

Andreadis, K. M., and D. P. Lettenmaier (2006), Assimilating remotely sensed snow observations into a macroscale hydrology model, *Adv. Water Resour.*, *29*, 872–886, doi:10.1016/j.advwatres.2005.08.004.

Armstrong, R., and M. Brodzik (2002), Hemispheric-scale comparison and evaluation of passive-microwave snow algorithms, *Ann. Glaciol.*, *34*, 38–44, doi:10.3189/172756402781817428.

Armstrong, R., M. J. Brodzik, and S. Arnault (Eds.) (1995), An earth-gridded SSM/I data set for cryospheric studies and global change monitoring, *Adv. Space Res.*, *16*(10) 155–163, doi:10.1016/0273-1177(95)00397-W.

Azar, E. A., H. Ghedira, P. Romanov, S. Mahani, M. Tedesco, and R. Khanbilvardi (2008), Application of satellite microwave images in estimating snow water equivalent, *J. Am. Water Resour. Assoc.*, *44*(6), 1347–1362, doi:10.1111/j.1752-1688.2008.00227.x.

Carroll, T., D. Cline, C. Olheiser, A. Rost, A. Nilsson, G. Fall, C. Bovitz, and L. Li (2006), NOAA's National Snow Analyses, *Proc. Western* Snow Conference, Las Cruces, NM, vol. 74. [Available at www.westernsnowconference.org/sites/westernsnowconference.org/PDFs/2006Carroll.pdf.]

Chang, A., J. Foster, and D. Hall (1996), Effects of forest on the snow parameters derived from microwave measurements during the Boreas winter field campaign, *Hydrol. Processes*, *10*, 1565–1574, doi:10.1002/(SICI)1099-1085(199612)10:12<1565::AID-HYP501>3.0.CO;2–5.

Chang, A., R. Kelly, E. Josberger, R. Armstrong, J. Foster, and N. Mognard (2005), Analysis of ground-measured and passive microwave-derived snow depth variations in midwinter across the Northern Great Plains, *J. Hydrometeorol.*, *6*, 20–33, doi:10.1175/JHM-405.1.

Chang, A. T. C., A. Foster, and D. Hall (1987), Nimbus-7 derived global snow cover parameters, *Ann. Glaciol.*, *9*, 39–44.

Clifford, D. (2010), Global estimates of snow water equivalent from passive microwave: History, challenges and future developments, *Int. J. Remote Sens.*, *31*(14), 3707–3726, doi:10.1080/01431161.2010.483482.

Clow, D., L. Nanus, K. Verdin, and J. Schmidt (2012), Evaluation of SNODAS snow depth and snow water equivalent estimates for the Colorado Rocky Mountains, USA, *Hydrol. Processes*, *26*, 2583–2591, doi:10.1002/hyp.9385.

Daly, S. F., R. Davis, E. Ochs, and T. Pangburn (2001), An approach to spatially distributed snow modeling of the Sacramento and San Joaquin basins, California, *Hydrol. Processes*, *14*, 3257–3271, doi:10.1002/1099-1085(20001230)14:18<3257::AID-HYP199>3.0.CO;2-Z.

Daly, S. F., C. Vuyovich, E. Deeb, S. Newman, T. Baldwin, and J. Gagnon (2012), Assessment of the snow conditions in the major watersheds of Afghanistan using multispectral and passive microwave remote sensing, *Hydrol. Processes*, *26*, 2634–2642, doi:10.1002/hyp.9367.

Derksen, C., A. Walker, and B. Goodison (2003), A comparison of 18 winter seasons of in situ and passive microwave-derived snow water equivalent estimates in Western Canada, *Remote Sens. Environ.*, *88*, 271–282, doi:10.1016/j.rse.2005.02.014.

Derksen, C., A. Walker, B. Goodison, and J. Strapp (2005), Integrating in situ and multiscale passive microwave data for estimation of subgrid scale snow water equivalent distribution and variability, *IEEE Trans. Geosci. Remote Sens.*, *43*(5), 960–972, doi:10.1109/TGRS.2004.839591.

Doesken, N. J., and A. Judson (1996), *The Snow Booklet: A Guide to the Science Climatology and Measurements of Snow in the United States*, 2nd ed., Colo. Clim. Cent., Fort Collins.

Dong, J., J. Walker, and P. Houser (2005), Factors affecting remotely sensed snow water equivalent uncertainty, *Remote Sens. Environ.*, *97*, 68–82, doi:10.1016/j.rse.2005.04.010.

Dozier, J. (2011), Mountain hydrology, snow color, and the fourth paradigm, *Eos Trans. AGU*, *92*, 373–375, doi:10.1029/2011EO430001.

Durand, M., E. J. Kim, S. A. Margulis, and N. P. Molotch (2011), A first-order characterization of errors from neglecting stratigraphy in forward and inverse passive microwave modeling of snow, *IEEE Trans. Geosci. Remote Sens.*, *8*(4), 730–734, doi:10.1109/LGRS.2011.2105243.

Farmer, C. J. Q., T. A. Nelson, M. A. Wulder, and C. Derksen (2010), Identification of snow cover regimes through spatial and temporal clustering of satellite microwave brightness temperatures, *Remote Sens. Environ.*, *114*, 199–210, doi:10.1016/j.rse.2009.09.002.

Foster, J., C. Sun, J. Walker, R. Kelly, A. Chang, J. Dong, and H. Powell (2005), Quantifying the uncertainty in passive microwave snow water equivalent observations, *Remote Sens. Environ.*, *94*, 187–203, doi:10.1016/j.rse.2004.09.012.

Foster, J., G. Skofronick-Jackson, H. Meng, J. Wang, G. Riggs, P. Kocin, B. Johnson, J. Cohen, D. Hall, and S. V. Nghiem (2012), Passive microwave remote sensing of the historic February 2010 snowstorms in the Middle Atlantic region of the USA, *Hydrol. Processes*, *26*, 3459–3471, doi:10.1002/hyp.8418.

Foster, J. L., D. K. Hall, A. T. C. Chang, A. Rango, W. Wergin, and E. Erbe (1999), Effects of snow crystal shape on the scattering of passive microwave radiation, *IEEE Trans. Geosci. Remote Sens.*, *37*, 1165–1168, doi:10.1109/36.752235.

Frankenstein, S., A. Sawyer, and J. Koeberle (2008), Comparison of FASST and SNTHERM in three snow accumulation regimes, *J. Hydrometeorol.*, *9*, 1443–1463, doi:10.1175/2008JHM865.1.

Guan, B., N. Molotch, D. Waliser, S. Jepsen, T. Painter, and J. Dozier (2013), Snow water equivalent in the Sierra Nevada: Blending snow sensor observations with snowmelt model simulations, *Water Resour. Res.*, *49*, 1–18, doi:10.1002/wrcr.20387.

Hall, D. K., A. T. C. Chang, and J. L. Foster (1986), Detection of the depth-hoar layer in the snow-pack of the Arctic coastal-plain of Alaska, USA, using satellite data, *J. Glaciol.*, *32*, 87–94.

Hallikainen, M. T., F. T. Ulaby, and M. Abdelrazik (1986), Dielectric-properties of snow in the 3 to 37 Ghz range, *IEEE Trans. Antennas Propag.*, *34*, 1329–1340, doi:10.1109/TAP.1986.1143757.
Hansen, M., R. DeFries, J. R. Townshend, M. Carroll, C. Dimiceli, and R. Sohlberg (2006), *Vegetation Continuous Fields MOD44B, 2001 Percent Tree Cover, Collection 4*, Univ. of Md, College Park.
Helsel, D. R., and R. M. Hirsch (2002), Statistical methods in water resources, *U.S. Geol. Surv. Tech. Water Resour. Invest., Book 4, Chap. A3*, 217 pp.
Jordan, R. (1990), *User's Guide for USACRREL One-Dimensional Snow Temperature Model (SNTHERM.89)*, U.S. Army Cold Reg. Res. and Eng. Lab., Hanover, N. H.
Josberger, E., N. Mognard, B. Lind, R. Matthews, and T. Carroll (1998), Snowpack water-equivalent estimates from satellite and aircraft remote-sensing measurements of the Red River basin, north-central U.S.A., *Ann. Glaciol.*, *26*, 119–124.
Josberger, E. G., and N. M. Mognard (2002), A passive microwave snow depth algorithm with a proxy for snow metamorphism, *Hydrol. Processes*, *16*, 1557–1568.
Kelly, R. (2009), The AMSR-E snow depth algorithm: Description and initial results, *J. Remote Sens. Soc. Jpn.*, *29*, 307–317.
Lea, J., and I. Reid (2006), An evaluation of the SNODAS for determining snow water equivalent on Mount St. Helens, Washington, paper presented at 74th Annual Western Snow Conference, Las Cruces, N. M.
Mätzler, C. (1987), Application of the interaction of microwaves with the natural snow cover, *Remote Sens. Rev.*, *2*(2), 259–287, doi:10.1080/02757258709532086.
Mätzler, C., and A. Standley (2000), Relief effects for passive microwave remote sensing, *Int. J. Remote Sens.*, *21*, 2403–2412, doi:10.1080/01431160050030538.
Meromy, L., N. P. Molotch, T. E. Link, S. R. Fassnacht, and R. Rice (2013), Subgrid variability of snow water equivalent at operational snow stations in the western USA, *Hydrol. Processes*, *27*, 2383–2400, doi:10.1002/hyp.9355.
Mizukami, N., and S. Perica (2012), Towards improved snow water equivalent retrieval algorithms for satellite passive microwave data over the mountainous basins of western USA, *Hydrol. Processes*, *26*, 1991–2002, doi:10.1002/hyp.8333.
Molotch, N. P., and R. C. Bales (2005), Scaling snow observations from the point to the grid-element: Implications for observation network design, *Water Resour. Res.*, *41*, W11421, doi:10.1029/2005WR004229.
Mote, T. L., A. J. Grundstein, D. J. Leathers, and D. A. Robinson (2003), A comparison of modeled, remotely sensed, and measured snow water equivalent in the northern Great Plains, *Water Resour. Res.*, *39*(8), 1209, doi:10.1029/2002WR001782.
Nash, J. E., and J. V. Sutcliffe (1970), River flow forecasting through conceptual models. Part I: A discussion of principles, *J. Hydrol.*, *10*, 282–290, doi:10.1016/0022-1694(70)90255-6.
Rittger, K., A. Kahl, and J. Dozier (2011), Topographic distribution of snow water equivalent in the Sierra Nevada, *Proc. Western Snow Conf., 79*, pp. 37–46. [Available at www.westernsnowconference.org/sites/westernsnowconference.org/PDFs/2011Rittger.pdf.]
Rutter, N., D. Cline, and L. Li (2008), Evaluation of the NOHRSC Snow Model (NSM) in a one-dimensional mode, *J. Hydrometeorol.*, *9*(4), 695–711, doi:10.1175/2008JHM861.1.
Schneiderman, E., A. Matonse, M. Zion, D. Lounsbury, R. Mukundan, S. Pradhanang, and D. Pierson (2013), Comparison of approaches for snowpack estimation in New York City watersheds, *Hydrol. Processes*, *27*, 3050–3060, doi:10.1002/hyp.9868.
Sturm, M., J. Holmgren, and G. E. Liston (1995), A seasonal snow cover classification system for local to global applications, *J. Clim.*, *8*(5), 1261–1283, doi:10.1175/1520-0442.
Tait, A. B. (1998), Estimation of snow water equivalent using passive microwave radiation data, *Remote Sens. Environ.*, *64*, 286–291, doi:10.1016/S0034-4257(98)00005-4.
Tedesco, M., and P. S. Narvekar (2010), Assessment of the NASA AMSR-E SWE product, *IEEE J. Selec. Top. Appl. Earth Observ. Remote Sens.*, *3*(1), 141–159, doi:10.1109/JSTARS.2010.2040462.
Todhunter, P. E. (2001), A hydroclimatological analysis of the Red River of the North snowmelt flood catastrophe of 1997, *J. Am. Water Resour. Assoc.*, *37*(5), 1263–1278, doi:10.1111/j.1752-1688.2001.tb03637.x.
Tong, J., S. Dery, P. Jackson, and C. Derkson (2010), Testing snow water equivalent retrieval algorithms for passive microwave remote sensing in an alpine watershed of western Canada, *Can. J. Remote Sens.*, *36*(1), S74–S86, doi:10.5589/m10-009.
USACE (2012), *Mississippi River and Tributaries System: 2011 Post-Flood Report*, Mississippi Valley Division, Vicksburg, Miss., December 2012.
Vander Jagt, B., M. T. Durand, S. A. Margulis, E. J. Kim, and N. P. Molotch (2013), The effect of spatial variability on the sensitivity of passive microwave measurements to snow water equivalent, *Remote Sens. Environ.*, *136*, 163–179, doi:10.1016/j.rse.2013.05.002.
Vuyovich, C., and J. Jacobs (2011), Snowpack and runoff generation using AMSR-E passive microwave observations in the Upper Helmand Watershed, Afghanistan, *Remote Sens. Environ.*, *115*, 3313–3321, doi:10.1016/j.rse.2011.07.014.
Walker, A., and B. Goodison (1993), Discrimination of a wet snow cover using passive microwave satellite data, *Ann. Glaciol.*, *17*, 307–311.